Government of Canada Gouvernement du Canada

Canada

# Numerical Prediction of Aerodynamic Performance of a Complete Aircraft with Contaminated Wings and Flaps

TP 14021E

June 1998

Prepared for

Transportation Development Centre
Transport Canada

by

National Research Council Canada
Institute for Aerospace Research
Aerodynamics Laboratory
Ottawa, Ontario

103-03486/

TP 14021E

# Numerical Prediction of Aerodynamic Performance of a Complete Aircraft with Contaminated Wings and Flaps

by
R.S. Crabbe and J. Su
National Research Council Canada
Institute for Aerospace Research
Aerodynamics Laboratory
Ottawa, Ontario

June 1998

This report reflects the views of the authors and not necessarily those of the Transportation Development Centre of Transport Canada.

The Transportation Development Centre does not endorse products of manufacturers. Trade or manufacturers' names appear in this report only because they are essential to its objectives.

Transport Canada / Transports Canada

# PUBLICATION DATA FORM

| 1. Transport Canada Publication No. | 2. Project No. | 3. Recipient's Catalogue No. |
|---|---|---|
| TP 14021E | 8786 (DC 129) | |

| 4. Title and Subtitle | 5. Publication Date |
|---|---|
| Numerical Prediction of Aerodynamic Performance of a Complete Aircraft with Contaminated Wings and Flaps | June 1998 |
| | 6. Performing Organization Document No. LTR-A-026 |
| 7. Author(s) R.S. Crabbe and J. Su | 8. Transport Canada File No. ZCD2450-B-14 |
| 9. Performing Organization Name and Address<br>National Research Council Canada<br>Institute for Aerospace Research<br>Aerodynamics Laboratory<br>Ottawa, Ontario<br>Canada K1A 0R6 | 10. PWGSC File No.<br>11. PWGSC or Transport Canada Contract No. |
| 12. Sponsoring Agency Name and Address<br>Transportation Development Centre (TDC)<br>800 René Lévesque Blvd. West<br>Suite 600<br>Montreal, Quebec<br>H3B 1X9 | 13. Type of Publication and Period Covered: Final<br>14. Project Officer: Barry B. Myers |

15. Supplementary Notes (Funding programs, titles of related publications, etc.)

Co-sponsored by Natural Research Council Canada's Institute for Aerospace Research (NRC/IAR)

16. Abstract

Numerical analyses have been carried out on the aerodynamics of a complete aircraft with contaminated wings and flaps. The numerical method is based on an interactive boundary layer approach that involves interaction between the inviscid potential and viscous boundary layer solutions. The potential flow is obtained by using a low-order panel method while the boundary layer solution is obtained by solving the three dimensional integral boundary layer equations in a streamline coordinate system. The rough surface skin-friction relations of Dvorak (1969), which incorporate both surface roughness height and density, are used to deal with the contamination effects. A computer code, PMAL3D, has been developed for carrying out the numerical calculations.

Predictions by PMAL3D are in very close agreement with experimental data for clean surface cases with or without ground effect. Computational results and discussion are further given for the influence of contamination on total lift of a configuration. In terms of total lift loss, PMAL3D predicts results in agreement with the experiment.

| 17. Key Words | 18. Distribution Statement |
|---|---|
| Aerodynamic modelling, contaminated take-off, aerodynamic behaviour, roughness, lift loss, flow separation | Limited number of copies available from the Transportation Development Centre |

| 19. Security Classification (of this publication) | 20. Security Classification (of this page) | 21. Declassification (date) | 22. No. of Pages | 23. Price |
|---|---|---|---|---|
| Unclassified | Unclassified | — | x, 20, app. | Shipping/ Handling |

Transports Canada Transport Canada

# FORMULE DE DONNÉES POUR PUBLICATION

| 1 N° de la publication de Transports Canada | 2 N° de l'étude | 3 N° de catalogue du destinataire |
|---|---|---|
| TP 14021E | 8786 (DC 129) | |

| 4 Titre et sous-titre | 5 Date de la publication |
|---|---|
| Numerical Prediction of Aerodynamic Performance of a Complete Aircraft with Contaminated Wings and Flaps | Juin 1998 |
| | 6 N° de document de l'organisme exécutant: LTR-A-026 |
| 7 Auteur(s): R.S. Crabbe et J. Su | 8 N° de dossier - Transports Canada: ZCD2450-B-14 |
| 9 Nom et adresse de l'organisme exécutant: Conseil national de recherches du Canada, Institut de recherche aérospatiale, Laboratoire d'aérodynamique, Ottawa, Ontario, Canada K1A 0R6 | 10 N° de dossier - TPSGC |
| | 11 N° de contrat - TPSGC ou Transports Canada |
| 12 Nom et adresse de l'organisme parrain: Centre de développement des transports (CDT), 800, boul. René-Lévesque Ouest, Bureau 600, Montréal (Québec), H3B 1X9 | 13 Genre de publication et période visée: Final |
| | 14 Agent de projet: Barry B. Myers |

15 Remarques additionnelles (programmes de financement, titres de publications connexes, etc.)

Coparrainé par l'Institut de recherche aérospatiale du Conseil national de recherches du Canada (CNRC/IRA)

16 Résumé


Des analyses numériques ont permis de caractériser les propriétés aérodynamiques d'un aéronef en vraie grandeur dont les ailes et les volets sont contaminés. La méthode d'analyse utilisée s'appuie sur une vision interactive de la couche limite, laquelle pose l'existence d'une interaction entre les solutions d'écoulement potentiel non visqueux et de couche limite visqueuse. La solution d'écoulement potentiel est obtenue à l'aide d'une méthode des panneaux d'ordre faible, tandis que celle de la couche limite découle de la résolution des équations intégrales tridimensionnelles de la couche limite, dans un système de coordonnées qui définit la ligne de courant. Les relations de Dvorak (1969) touchant la traînée due au frottement, qui font intervenir l'épaisseur et la densité des rugosités de la surface, ont servi à l'étude des effets de la contamination. Enfin, un code machine, le PMAL3D, a été mis au point aux fins des calculs numériques.

Les prévisions faites à l'aide du PMAL3D sont étroitement corrélées avec les résultats d'expériences réalisées sur des surfaces propres, avec ou sans effet de sol. Le rapport contient également des résultats de calculs assortis de commentaires sur les effets de la contamination sur la portance totale d'une configuration. Pour ce qui est de la perte de portance totale, les résultats issus du code PMAL3D concordent avec les données expérimentales.


| 17 Mots clés | 18 Diffusion |
|---|---|
| Modélisation aérodynamique, décollage d'un aéronef contaminé, comportement aérodynamique, rugosité, perte de portance, séparation de l'écoulement | Le Centre de développement des transports dispose d'un nombre limité d'exemplaires. |

| 19 Classification de sécurité (de cette publication) | 20 Classification de sécurité (de cette page) | 21 Déclassification (date) | 22 Nombre de pages | 23 Prix |
|---|---|---|---|---|
| Non classifiée | Non classifiée | — | x, 20, ann. | Port et manutention |

## ACKNOWLEDGEMENTS

This work was supported by Transport Canada. The authors wish to thank Messrs. Frank Eyre and Barry Myers of the Transportation Development Centre for their helpful discussions and cooperation.

## TABLE OF CONTENTS

Introduction ..... 1

Methodology ..... 2

Case Studies ..... 4

Conclusions and Recommendation ..... 6

References ..... 7

Appendix A

## LIST OF FIGURES


Figure 1 Representation of the geometry of Fokker F28 M1000 aircraft by surface panels..... 9

Figure 2 Lift coefficient of Fokker F28 M1000 configuration with 18 deg flap deflection. $U_\infty = 70$ m s$^{-1}$; free air with no ground effect ..... 10

Figure 3 Lift coefficient of Fokker F28 with 18 deg flap deflection. $U_\infty = 57.8$ m s$^{-1}$; ground effect included with and without roughness; roughness height $k = 1.0$ mm, roughness density parameter $\lambda = 5.0$ ..... 11

Figure 4 Comparison of the lift coefficient of F28 with clean and contaminated wing/flap. $k = 1.0$ mm, $\lambda = 5.0$ ..... 12

Figure 5 Comparison of the lift coefficient of F28 with different roughness heights and densities ..... 13

Figure 6 Influence of leading and trailing edge contaminations on the lift coefficient of F28 ..... 14

Figure 7 Influence of leading and/or trailing edge contaminations on the lift coefficient of F28. $k = 1.0$ mm, $\lambda = 5.0$ ..... 15

Figure 8 Effect of practical contamination conditions on the lift coefficient ..... 16

Figure 9 Influence of laminar/turbulent transition on the lift coefficient (no roughness) ..... 17

Figure 10 An assumed contamination pattern for roughness studies ..... 18

Figure 11 A practical contamination pattern with 20% failure. A-D: $k = 1.0$ mm, $\lambda = 8.0$; E: $k = 0.5$ mm, $\lambda = 50.0$ ..... 18

Figure 12 A practical contamination pattern with 75% failure. A-C: $k = 1.0$ mm, $\lambda = 8.0$; E-H: $k = 0.2$ mm, $\lambda = 800.0$; I: $k = 0.4$ mm, $\lambda = 50.0$; D, J: $k = 0.5$ mm, $\lambda = 35.0$ ..... 19

Figure 13 A practical case of snow deposit on a parked F28 M1000 aircraft ..... 20

## LIST OF SYMBOLS

$C_f$ = skin-friction coefficient

$C_L$ = lift coefficient

$e$ = entrainment constant

$H$ = shape factor of streamwise velocity profile, $\delta_1^* / \theta_{11}$

$H_{\delta-\delta_1^*}$ = entrainment shape factor of streamwise velocity profile, $(\delta - \delta_1^*)/\theta_{11}$

$k$ = roughness height

$n$ = crossflow coordinate

$s$ = streamline coordinate

$u$ = streamwise boundary-layer velocity component

$U$ = resultant velocity at boundary layer edge

$U_\infty$ = undisturbed freestream velocity

$v$ = crossflow boundary-layer velocity component

$\alpha$ = angle of attack

$\beta$ = angle between an external streamline and corresponding limiting streamline

$\gamma$ = streamline direction with respect to $x$

$\delta$ = boundary layer thickness

$\delta_1^*, \delta_2^*$ = streamwise and crossflow displacement thicknesses

$\lambda$ = roughness density parameter

$\theta_{ij}$ = boundary layer momentum thicknesses

$\zeta$ = coordinate in the normal direction to surface

## INTRODUCTION

A number of fatal aircraft accidents during the last 15 years, occurring at take-off during periods of freezing precipitation, have directed considerable attention to the investigation of roughness effects of contamination on the aerodynamic performance of aircraft (Luers, 1983, Boer, 1991 and Kind and Lawrysyn, 1992). Protection of aircraft surfaces against adhesion and accumulation of freezing precipitation is currently achieved by application of freezing point depressant fluids (anti-icing fluids) for the brief period of taxi and take-off. In practice, take-off occurs when the pilot is satisfied that the critical surfaces are free from contamination. The practical method to accomplish this is by visual inspection, which is frequently difficult due to aircraft geometry and/or adverse lighting conditions. Under these circumstances it is possible that take-off may be attempted with surfaces that are contaminated by the adhesion of freezing precipitation which passed undetected or were non-existent at the time of pilot's final inspection. The contamination may not be uniform. Recent investigations into aircraft accidents where freezing precipitation buildup on the surfaces was deemed to be a factor, have assumed that the ground effect on aircraft aerodynamics was also a factor. The present work has investigated the influence of contamination on the aircraft aerodynamic performance with ground effect included.

Research work has been being carried out on this issue for several years at the Aerodynamics Laboratory, IAR/NRC. A two-dimensional computer code was first developed by Crabbe (1995), and later extended to three-dimensional wings (Crabbe, 1998) resulting in an earlier version of PMAL3D. PMAL3D has been shown (Crabbe, 1998) to predict inviscid wing lift to the accuracy of a commercial panel code, PMARC, which is to be expected inasmuch as both methods are low order using uniform source and doublet distributions on each surface panel. PMARC, which has been applied to compute inviscid flow about a complete aircraft (Edge and Perkins, 1995), is the potential portion of an earlier commercial code VSAERO. VSAERO contains a boundary layer code (for clean surfaces) that is specialized to the swept wing of infinite span. Consequently, it is only approximately valid for finite-span-wing aircraft. PMAL3D. On the other hand, it predicts viscous flow about general aircraft configurations with or without contaminated surfaces. Navier-Stokes solutions for multi-element airfoils and wings have been reported in the literature (e.g. Cebeci, 1997). While these methods automatically include viscous effects, the authors are not aware of any Navier-Stokes code that will treat three-dimensional aircraft surfaces with arbitrarily distributed roughness. Results reported in this paper demonstrate, however, that interactive panel codes, such as PMAL3D, can be readily adapted to aircraft surfaces with arbitrary patterns of both roughness height and spacing. PMAL3D not only predicts lift coefficients up to the onset of stall but can also predict the effect of slideslip on wing lift. However, this paper discusses the pre-stall lift loss of the wing-flap-fuselage-tail configuration of the F28M1000 aircraft due to roughness in coordinated flight.

## METHODOLOGY

In the viscous-inviscid interaction technique, separate calculations of the inviscid outer flow and the viscous inner flow are matched by an iterative procedure to yield a solution to the problem. The numerical method used in the present work employs this technique and involves interaction between the inviscid potential solution for the outer flow and the boundary layer solution for the inner flow. A potential solution is obtained by using a panel method while the boundary layer solution is obtained by solving three-dimensional integral boundary layer equations. This method has been demonstrated to be very efficient with little loss in accuracy for a broad range of applications to the external aerodynamics of aircraft.

Integral prediction methods for three-dimensional turbulent boundary layers are most readily described in a streamline coordinate system ($s$, $n$) on the body surface with $s$ being in the streamwise direction and $n$ being the normal direction to the streamline. The integral equations in this coordinate system are

*s momentum integral equation:*

$$\frac{\partial \theta_{11}}{\partial s}+\frac{\partial \theta_{12}}{\partial n}+\frac{\theta_{11}}{U}\frac{\partial U}{\partial s}(2+H)+\frac{\partial \gamma}{\partial n}(\theta_{11}-\theta_{22})=\frac{C_f}{2} \tag{1}$$

*n momentum integral equation:*

$$\frac{\partial \theta_{21}}{\partial s}+\frac{\partial \theta_{22}}{\partial n}+\frac{2}{U}\frac{\partial U}{\partial s}\theta_{21}+\frac{\theta_{11}}{U}\frac{\partial U}{\partial n}(1+H+\frac{\theta_{22}}{\theta_{11}})+2\frac{\partial \gamma}{\partial n}\theta_{21}=\frac{C_f}{2}\tan\beta \tag{2}$$

*entrainment equation:*

$$\frac{\partial(\delta-\delta_1^*)}{\partial s}-\frac{\partial \delta_2^*}{\partial n}=F(H_{\delta-\delta_1^*})-(\delta-\delta_1^*)[\frac{\partial U}{U\partial s}+\frac{\partial \gamma}{\partial n}(1-e)] \tag{3}$$

where $\partial\gamma/\partial n$ is streamline divergence. Crabbe (1977) has shown that $e=0.5$ in diverging flow ($\partial\gamma/\partial n>0$) and 0.1 in converging flow ($\partial\gamma/\partial n<0$). $F(H_{\delta-\delta_1^*})$ is Head's entrainment function. The displacement and momentum thicknesses are given by

$$\delta_1^*=\int_0^\delta(1-\frac{u}{U})d\zeta, \qquad \delta_2^*=-\int_0^\delta\frac{v}{U}d\zeta$$

$$\theta_{11}=\int_0^\delta\frac{u}{U}(1-\frac{u}{U})d\zeta, \qquad \theta_{12}=\int_0^\delta\frac{v}{U}(1-\frac{u}{U})d\zeta$$

$$\theta_{21}=-\int_0^\delta\frac{uv}{U^2}d\zeta, \qquad \theta_{22}=-\int_0^\delta\frac{v^2}{U^2}d\gamma \tag{4}$$

Mager's form for the crossflow

$$\frac{u}{v} = \left(1 - \frac{\zeta}{\delta}\right)^2 \tan\beta$$

and Cumsty and Head's form for the streamwise velocity profile,

$$\frac{u}{U} = \left(\frac{\zeta}{\delta}\right)^{\frac{H-1}{2}} \tag{5}$$

are used here. Equations (4) and (5) enable the crossflow integral thicknesses to be simply expressed as functions of $H$, $\theta_{11}$, and tan $\beta$.

The roughness effect of the contamination is simulated using the formulation developed by Dvorak (1969). In the present paper, the method has been applied to a complete aircraft where the main lifting surfaces (wing and flap) are contaminated by distributed roughness which arises when applications of anti-icing fluid fail to prevent local adhesion of freezing precipitation to these surfaces. The equation for the skin friction coefficient is expressed in terms of roughness height $k$ and dimensionless spacing $\lambda$ as

$$C_f = C_f(H, \theta_{11}, k, \lambda) \tag{6}$$

The details of this equation are given in Dvorak (1969).

The numerical integration of the above equation set is implemented along streamlines. Each streamline is divided into N subdivisions (25 for the wing and 15 for the flap for the results presented in this paper). Each subdivision is divided into four equal sections. A fourth order Runge-Kutta method is used to advance the numerical solution to the three-fourths point. The solution is then advanced to the end of the subdivision using the Adams-Bashforth-Moulton predictor-corrector method. The overall scheme is therefore a mix of explicit and implicit operations and has proven to be efficient and robust. Equations (1) to (3) are solved using the above scheme along two streamlines, one on each of the upper and lower surfaces of the wing or flap, in each of the chordwise strips, starting at the flow attachment line. Two nested computational loops are used. The outer loop is between the potential flow solution and the boundary layer flow solution while the inner loop for the boundary layer flow begins by ignoring orthogonal derivatives of the crossflow integrals and then follows by including them in the second and higher iterations.

## CASE STUDIES

Figure 1 shows the geometry of a Fokker F28 MI000 aircraft and the surface paneling used in the calculations. In total, 1740 panels are used for the half-configuration with 710 panels covering the wing and flap. The tail-fin is not included since its aerodynamic influence is negligible for a symmetric aircraft configuration under zero sideslip angle investigated here.

The lift coefficient of the Fokker F28 is presented in Figure 2. The upstream flow speed is equal to 70 m $s^{-1}$; Reynolds number at the mean chord is 17.5 million and no ground effect is included (free air). It has been shown that the potential solution obtained by PMAL3D is in very good agreement with the PMARC potential solution in Crabbe (1998). With the three-dimensional boundary layer included, PMAL3D therefore yields results close to the experimental data with clean surfaces (Morgan et al, 1989). The wing root angle of attack is 3.7 degrees higher than that of the fuselage (reference) angle of attack which is used in the second and subsequent figures, but the wing is twisted so that the tip flies at an angle of attack 3.9 degrees lower than the root.

Figure 3 shows similar results in ground effect. The upstream flow speed is 57.8 m $s^{-1}$; Reynolds number at the mean chord is 14.5 million. The leading edge of the root chord of the gross wing is two meters above ground. These conditions are close to the take-off scenario of the Fokker F28 M1000. Again the lift coefficient calculated by PMAL3D is in excellent agreement with the clean surface experimental data (Morgan et al, 1989). The roughness result obtained by simulating a contaminated wing and flap by PMAL3D is also presented in Figure 3. It is assumed that the whole wing upper surface and that part of the flap upper surface not hidden by the wing planform are contaminated. The roughness height is $k$ =1.0 mm and density parameter (nondimensional roughness spacing), $\lambda$ =5.0. An example of the use of $k$ and $\lambda$ to specify the physical properties of surface roughness is given in the appendix. Use of $k$ =1.0 mm with $\lambda$ =5.0 is a very severe contamination case at take-off. It is seen that even at a small angle of attack (0.0-6.0 degrees) without flow separation the lift of the configuration drops by about 10%. Obviously, the contamination effect is quite substantial for this case. The results for $k$ =1.0 mm and $\lambda$ =50.0 (lower roughness density than that with $\lambda$ =5.0) are given in Figure 4. Oleskiw and Penna (1997) have done wind tunnel measurements for a similar wing/flap configuration. The roughness condition for this case is quite close to the wind tunnel test carried out by them. From Figure 4, it is observed that the lift coefficient is reduced by about 5% by the roughness. This is quite a reasonable estimate of the effect of a rough surface on the lift according to the experimental data of Oleskiw and Penna (1997).

The results with different roughness heights and/or density parameters are presented in Figure 5. It is observed that the reduction in lift coefficient is not linearly related to $k$ and/or $\lambda$. For instance, increasing $k$ from 1.0 mm to 1.5 mm has not resulted in decreasing the lift coefficient significantly. In fact, the difference is quite small. However, further numerical investigation is required before a sound conclusion can be made.
In most practical situations, the contamination is localized at leading and/or trailing edges. Numerical results are also performed for this type of distribution. Figure 6 presents the results with 10% leading and 10% trailing edge contamination as shown in Figure 10. The roughness

height is $k$=1.0 mm and the density parameter $\lambda$=5.0. At angles of attack less than 2.0 degrees, the roughness of contamination has a very small effect on the lift. As the angle of attack increases the effect increases and at 6.0 degrees the lift is reduced by about 6%. The predictions with leading or trailing edge contamination alone are given in Figure 7. It is noticed that with either leading or trailing edge contamination the roughness effect is quite small; but the combination of them has greater influence on the lift. This result may mean that it is the total area of contamination that matters as long as there is no flow separation occurring.

For a typical contamination condition with 20% failure at take-off shown in Figure 11, the numerical prediction is given in Figure 8. It is evident that the roughness effect of the contamination is negligible up to 4.0 degrees of angle of attack. The numerical result for a contamination condition with 75% failure (Figure 12) is also presented in Figure 8. The difference between 20% and 75% failures is negligible.

Results were also computed for the practical case of the effect of snow on the lift characteristics of the F28 aircraft parked in a crosswind. The contaminant pattern for the leeward wing is shown in Figure 12. The contaminant pattern for the windward wing is not shown since it is only involves the lift spoilers where the roughness height is essentially 0.65 mm (compared with 1.0 mm on the leeward wing). The lift curves in take-off configuration (flap deflected 18 degrees from its stowed position) for the clean and contaminated aircraft are plotted on Figure 13 where it is seen that they are almost identical up to an angle of attack of six degrees. The maximum lift coefficients of the contaminated wings occur at 7.53 degrees where the lift coefficient of the leeward wing is slightly less than that of the windward wing, 1.509 vs. 1.510. This difference gives rise to a negligible rolling moment coefficient of $-3\times10^{-7}$ which is easily offset by aileron deflection. The overall effect on lift of this roughness pattern is small since the computed boundary-layer thickness in the region of maximum roughness height is 16 cm., or about 160 times the roughness height, at eight degrees angle of attack. Moreover, some of the snow could be expected to blow off during take-off thereby reducing the lift loss.

The roughness effect of contamination has been discussed above without flow separation occurring. However, the contamination may trigger earlier separation than without contamination, which could subsequently reduce the total lift of the configuration significantly even for the case shown in Figure 11. Thus, flow separations induced by contamination should be investigated for more comprehensive discussion of roughness effect of contamination. PMAL3D at the present stage of development can only handle cases without separated flow, although it does predict the boundary-layer separation line. (Cumpsty and Head, 1967, and Crabbe, 1998). Further extension to separated flows is obviously of importance for both practical applications and research purposes.

PMAL3D can also model a laminar boundary layer with a criterion for laminar/turbulent transition following the approach of Cebeci and Bradshaw (1977). The result with laminar/turbulent transition is compared with the fully turbulent result in Figure 9. It is noticed that the difference is negligible. Therefore approximating the whole boundary layer as being turbulent is reasonable for the configuration examined here.

## CONCLUSIONS AND RECOMMENDATION

A numerical method and discussions of its results have been presented on the aerodynamics of Fokker F28M1000 aircraft with contaminated wings and flaps. A computer code, PMAL3D, has been developed for carrying out the numerical calculations.

Predictions by PMAL3D are in very close agreement with experimental data for clean surface cases with or without the ground effect. The influence of contamination on total lift of the F28M1000 aircraft is discussed by choosing different contamination patterns with different roughness parameters. It is noticed that under certain conditions, even at small angles of attack and without separation, the roughness effect of contamination on the aerodynamics of aircraft can be significant. In terms of total lift loss, the PMAL3D prediction is very promising according to the experimental data of Oleskiw and Penna (1997).

The roughness effect of contamination without flow separation has been studied in this report. For more comprehensive analyses the separations induced by contamination should be investigated.

## REFERENCES


Boer, N., 1991, "Effect of Hoar-Frosted Wings on Fokker 50 Take-Off Characteristics," *AGARD 68th Fluid Dynamics Panel Specialists Meeting on Effects of Adverse Weather on Aerodynamics,* Toulouse, France.

Cebeci, T., 1997, "An Efficient and Accurate Approach for Analysis and Design of High Lift Configurations," *Proceedings of the 6th Aerodynamics Symposium,* April 28-30, Toronto, Ontario, Canada, pp. 65-80.

Cebeci, T. and Bradshaw, P., 1977, *Momentum Transfer in Boundary Layers,* Hemisphere Publishing Corporation, London, pp. 281-314.

Crabbe, R.S., 1977, "A Contribution to the Study of Uniformly Diverging and Converging Turbulent Boundary Layers," Ph.D Disssertion, McGill Univ., Montreal. PQ, Canada.

Crabbe, R.S., 1995, "Predicted Influence of Surface Roughness Including Fluid-Runback Waves on Airfoil Lift and Drag," *Report LTR-A-002,* IAR/NRC.

Crabbe, R.S., 1998, "A Simple Numerical Method to Compute Viscous Lift Loss of Wings," *Journal of Aircraft,* Vol.35, No.I, pp. 27-32.

Cumsty, N.A. and Head, M.R., 1967, "The Calculation of Three-Dimensional Turbulent Boundary Layers," *The Aeronautical Quarterly,* February, pp. 55-84.

Dvorak, F.A., 1969, "Calculation of Turbulent Boundary Layers on Rough Surfaces in Pressure Gradient," AIAA *Journal,* Vol. 7, No. 9, pp 1752-1759.

Edge D.C. and Perkins, J.N., 1995, "Three-Dimensional Aerodynamic Analysis of a Subsonic High-Lift Transport Configuration Using PMARC," AIAA *95-0039.*

Luers, J.K., 1983, "Wing Contamination: Threat to Safe Flight," *Astronautics and Aeronautics,* pp. 54-59.

Kind, R.J. and Lawrysyn, M.A., 1992, "Performance Degradation due to Hoar Frost on Lifting Surfaces," *Canadian Aeronautics and Space Journal,* Vol. 38, No.2.

Morgan, J.M., Wagner, G.A., and Wickens, R.H., 1989, "A Report on the Flight Dynamics of the Fokker F-28 Mk1000 as They Pertain to the Accident at Dryden, Ontario, March, 1989," Appendix 4 of the Final Report, Commission of Inquiry into the Air Ontario Crash at Dryden, Ontario. The Honourable Virgil P. Moshansky, Commissioner.

Oleskiw, M. M. and Penna, P.J., 1997, "Wind Tunnel Wing Section Performance with De/Anti-Icing Fluids and Freezing Precipitation," *SAE Aircraft Ground Deicing Conference,* Pittsburgh, Pennsylvania, June 11-13.

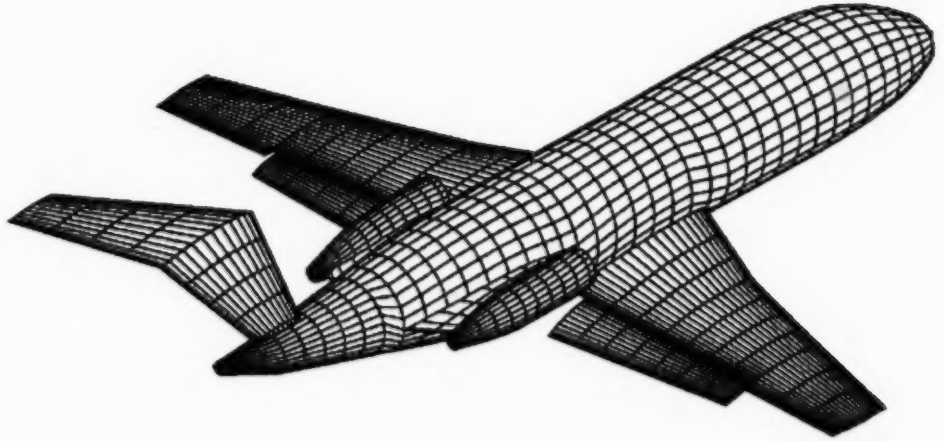

Figure 1 Representation of the geometry of the Fokker F28 M1000 aircraft by surface panels.

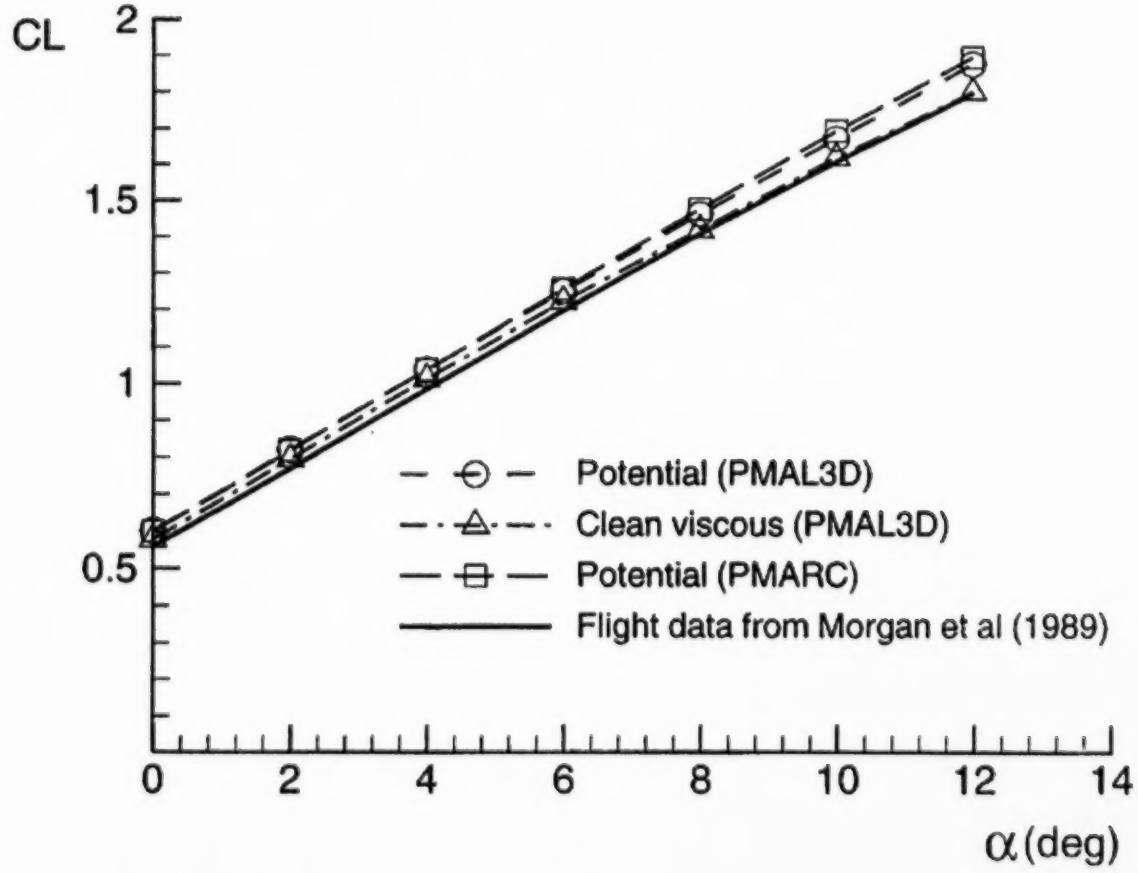


Figure 2 Lift coefficient of the Fokker F28 with an 18 deg flap deflection Free air with no roughness.

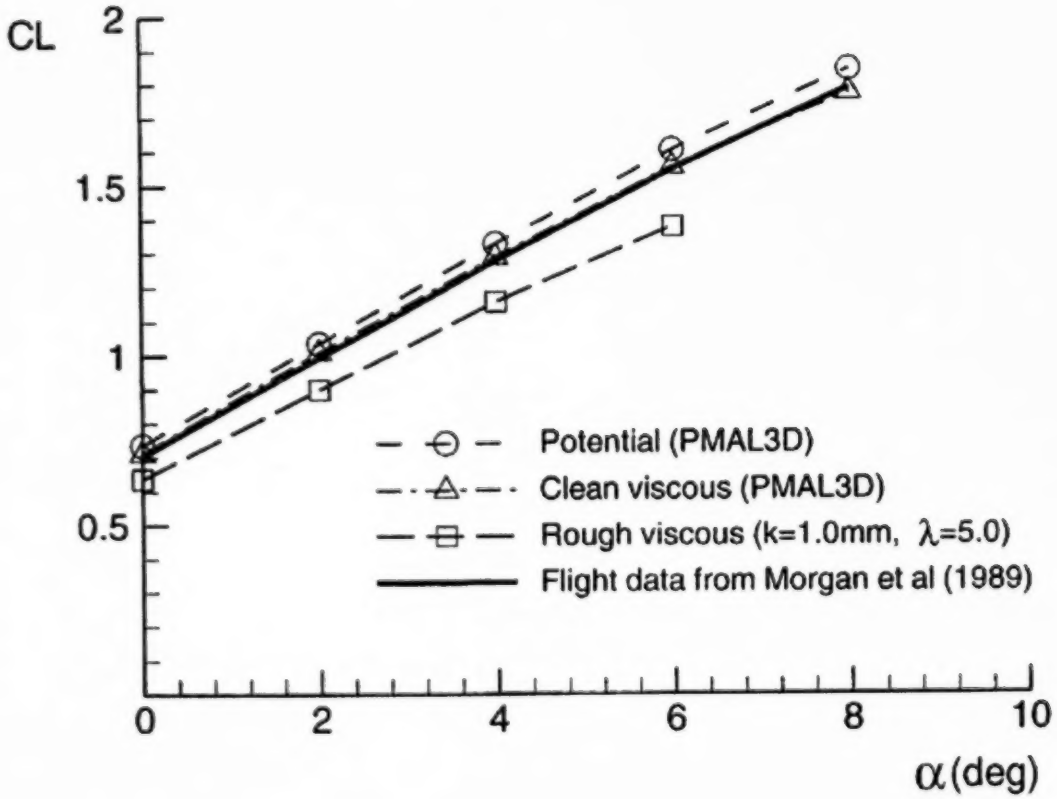


Figure 3 Lift coefficient of the Fokker F28 with an 18 deg flap deflection. Ground effect with and without roughness.

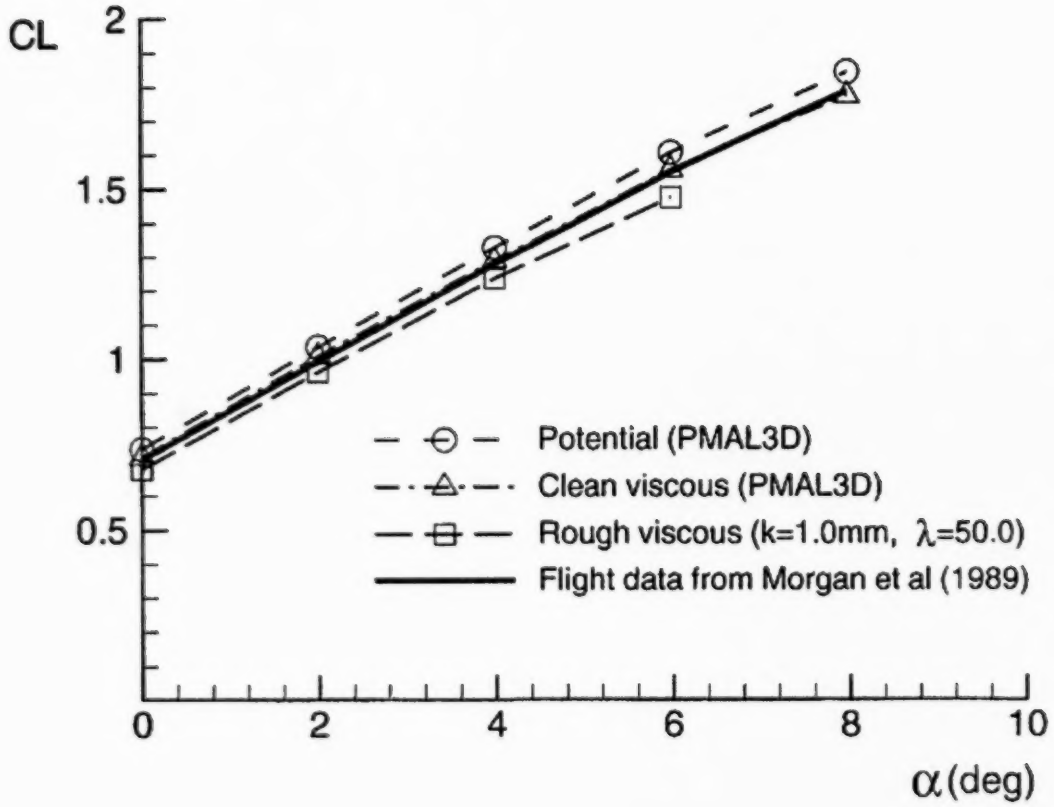


Figure 4 Comparison of the lift coefficient of the F28 with clean and contaminated wing/flap.

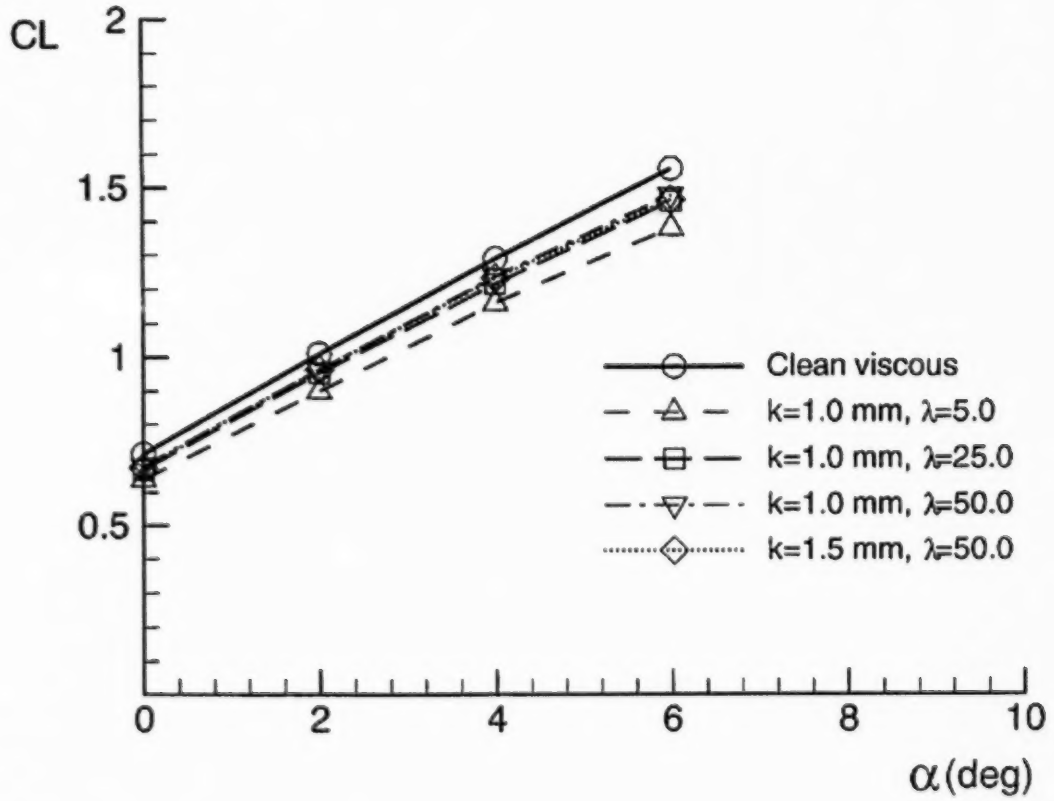


Figure 5 Comparison of the lift coefficient of the F28 with different roughness heights and densities.

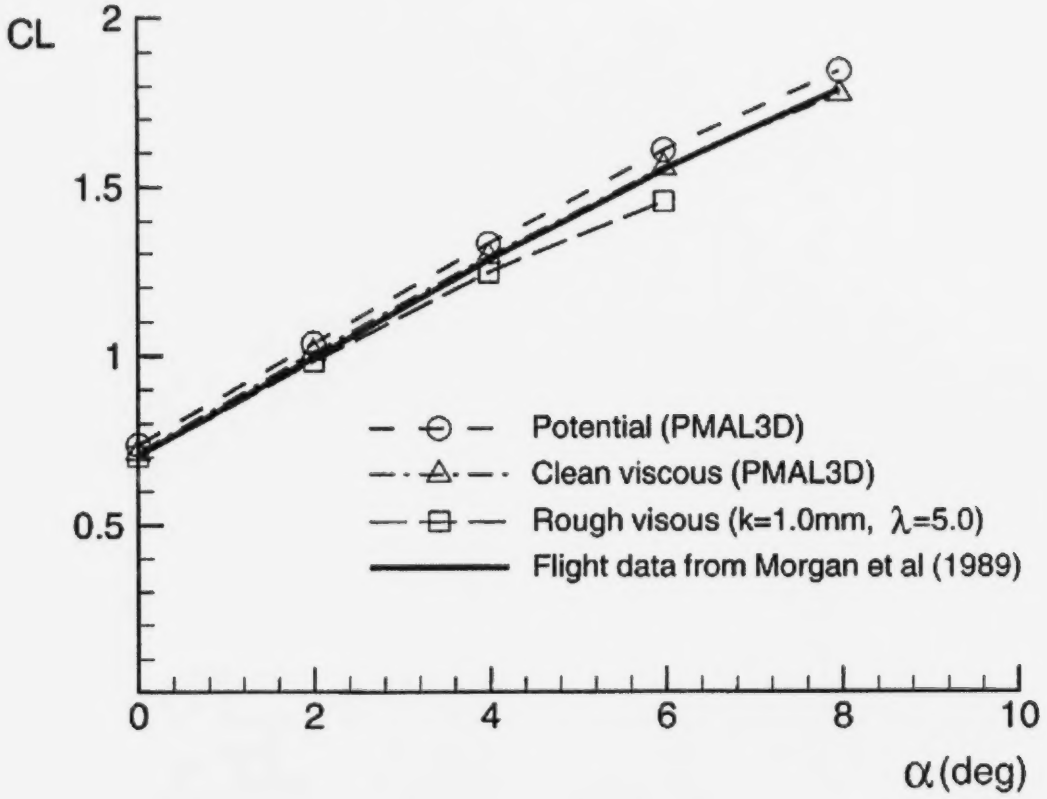


Figure 6 Influence of leading and trailing edge contamination on the lift coefficient of the F28.

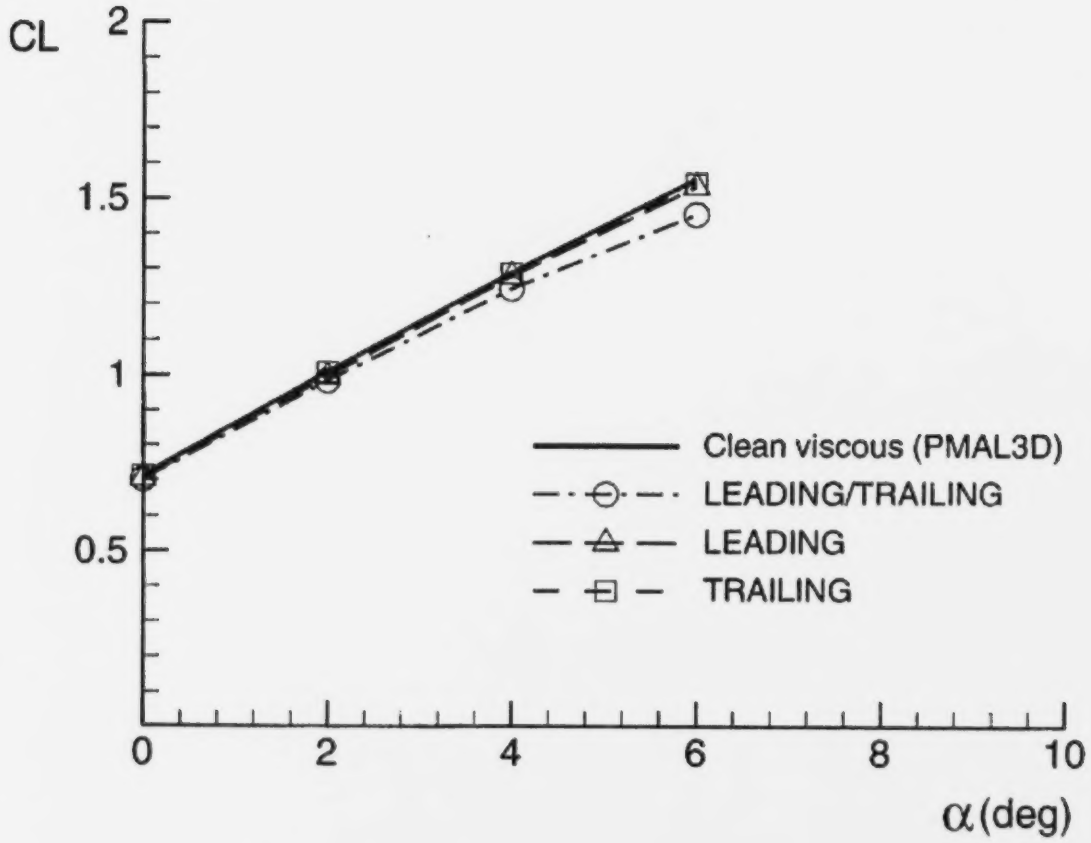


Figure 7 Influence of leading and/or trailing edge contamination on the lift coefficient of the F28 (k=1.0mm, $\lambda$=5.0).

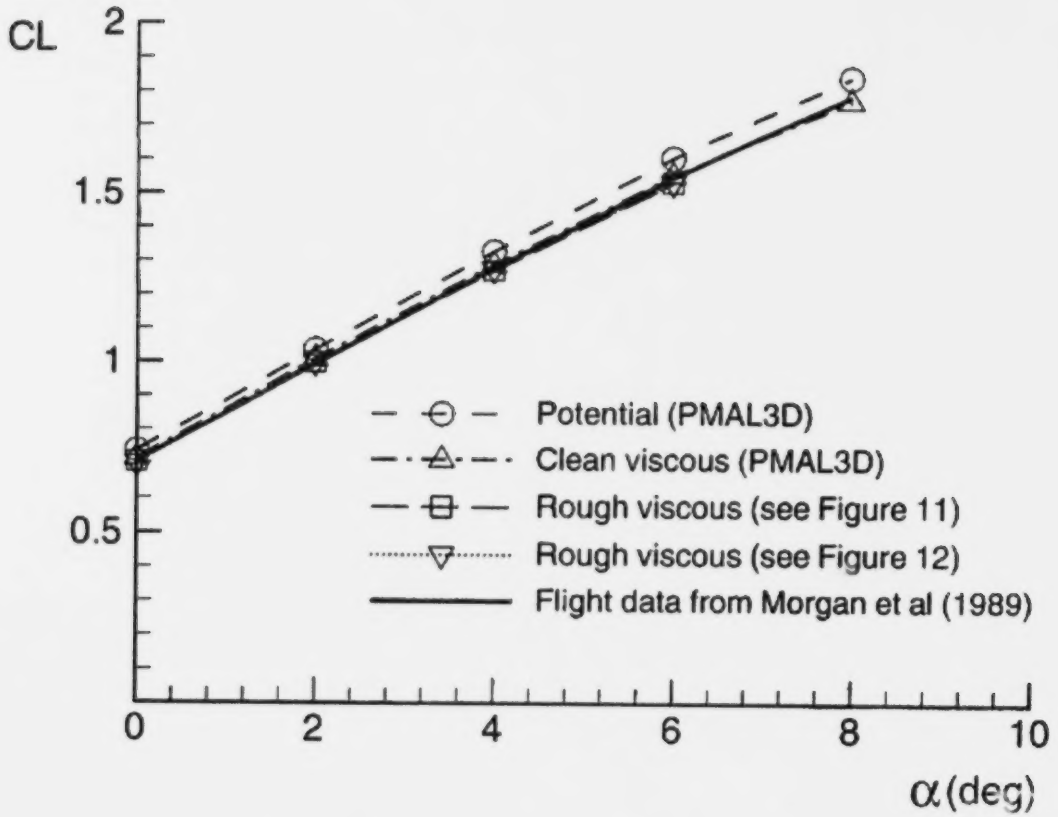


Figure 8 Effect of practical contamination conditions on the lift coefficient of the F28.

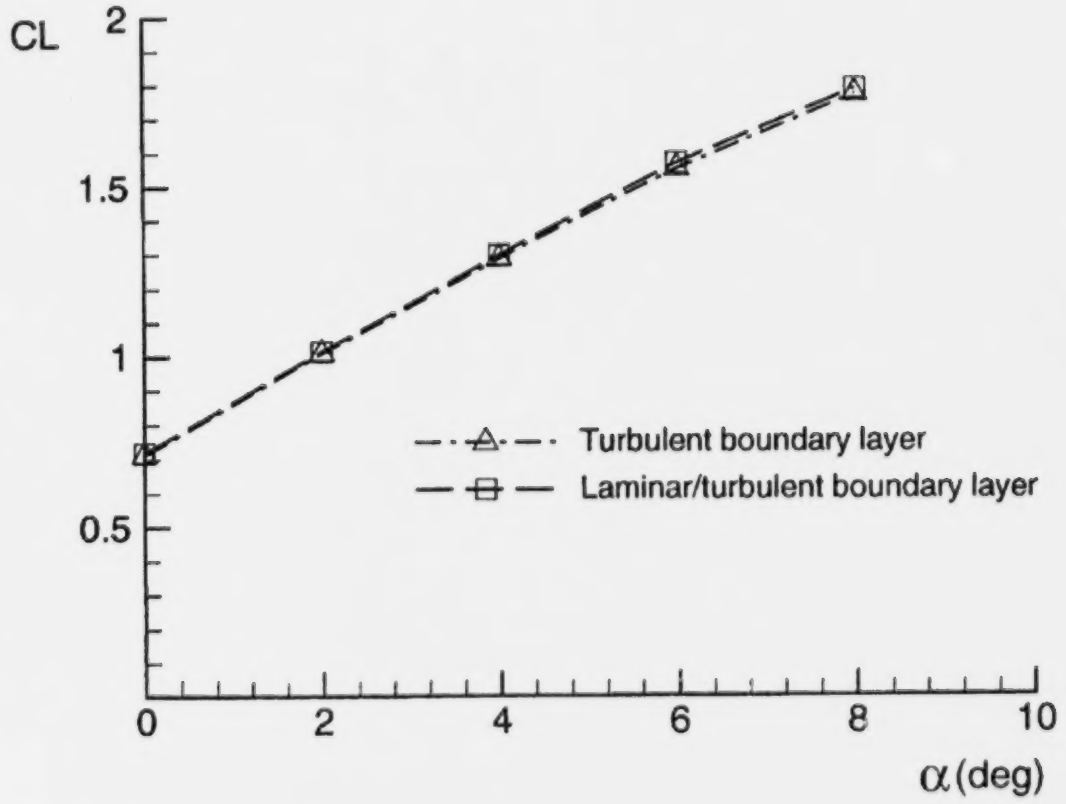


Figure 9 Influence of laminar/turbulent transition on the lift coefficient (no roughness).

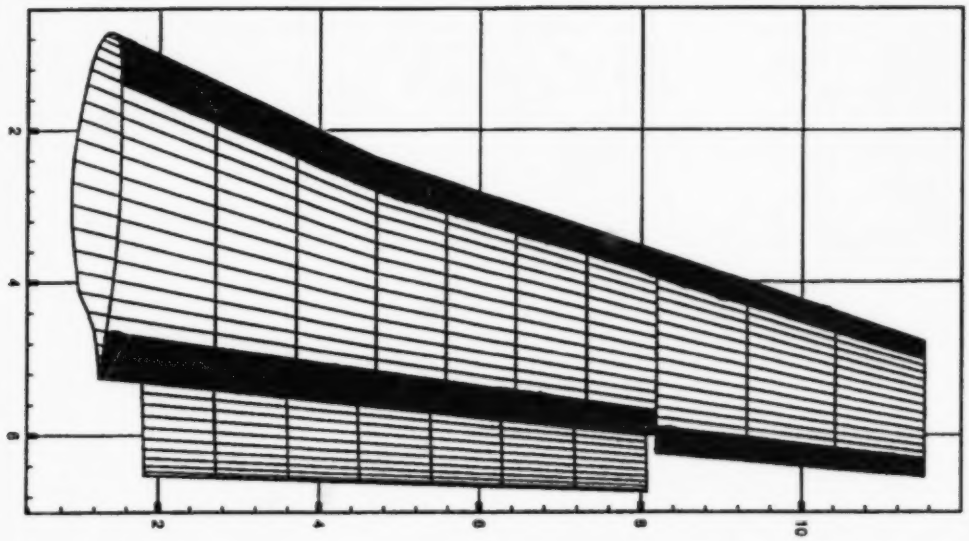

Figure 10 An assumed contamination pattern for roughness studies.

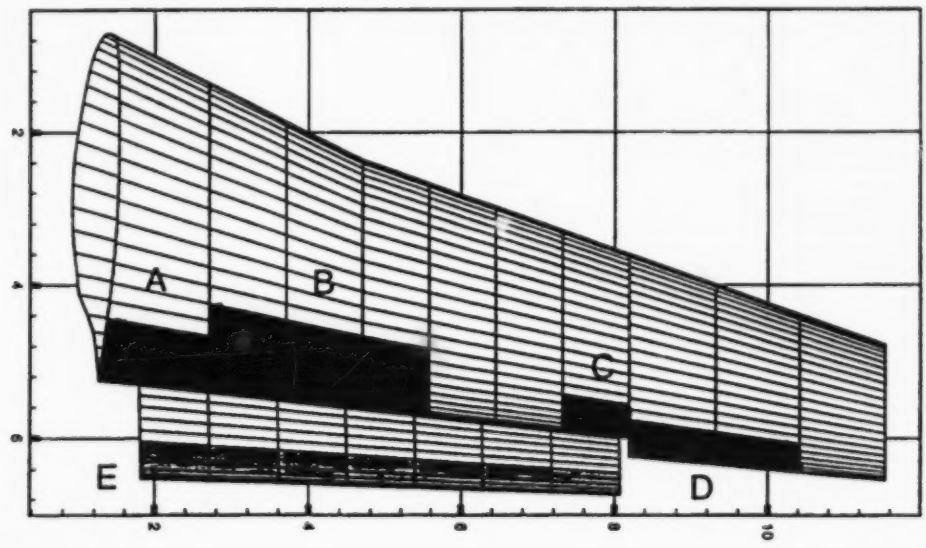


Figure 11 A practical contamination pattern with 20% wing failure.
A-D: k=1.0mm, $\lambda$=8.0; E: k=0.5mm, $\lambda$=50.0.

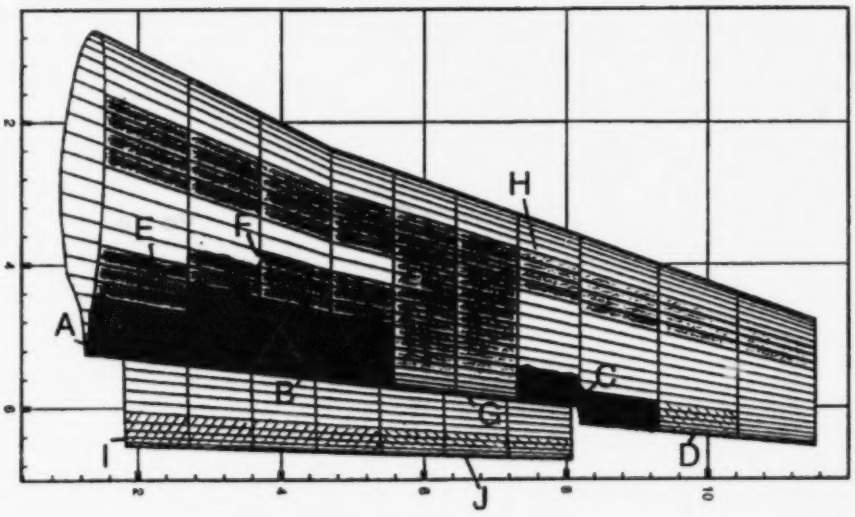


Figure 12 A practical contamination pattern with 75% wing failure.
A-C: k=1.0mm, $\lambda$=8.0; E-H: k=0.2mm, $\lambda$=800.0; I: k=0.4mm,
$\lambda$=50.0; D, J: k=0.5mm, $\lambda$=35.0.

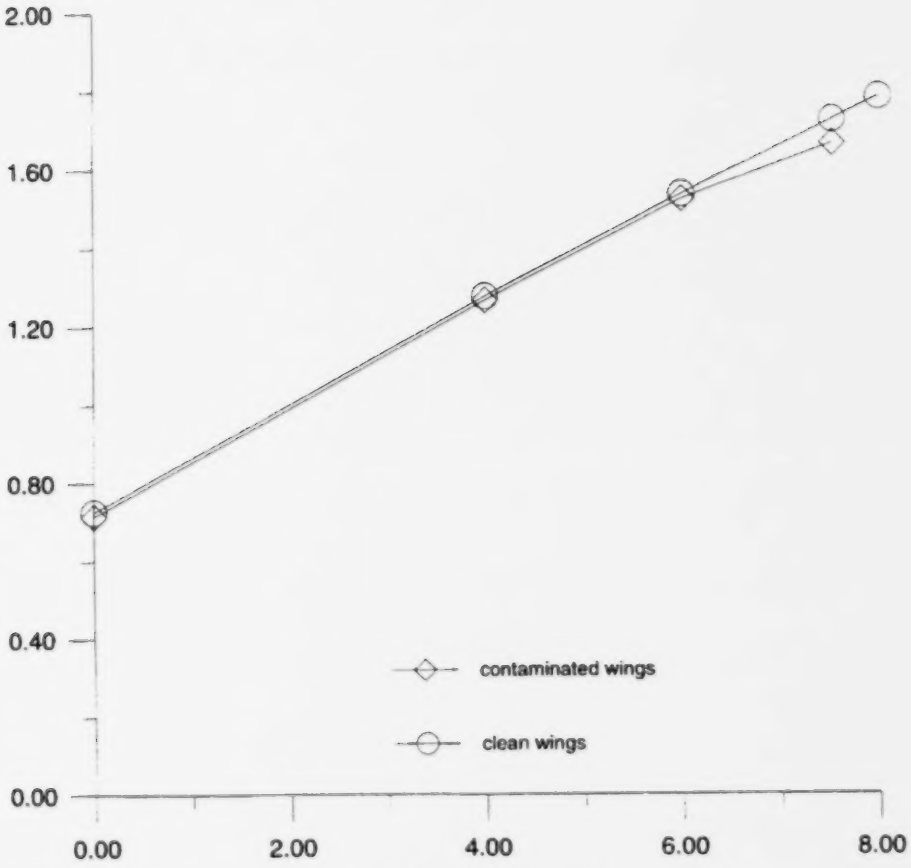


Figure 13

Lift curve of the F28 with light snow deposit on the wings

## Appendix A

The simplest method of specifying the physical properties of surface roughness is in terms of the roughness height, $k$, the average frontal area of a roughness element, $A_F$, the average area occupied by a roughness element, $D^2$ and the average non-dimensional separation between elements, $\lambda = D^2/ A_F$. $D^2$ is easily estimated by counting the number of elements in a given roughness area while $A_F$ is assumed to scale with the square of the roughness height. Thus, $A_F = ak^2$ where a is itself a combination of factors accounting for the ratio of the average height to the height of the highest 20% of the elements and the average width-to-height ratio of the elements. Overall, a is about 1.0 so that the average spacing, or density of the roughness pattern, in the simplest case is $\lambda = D^2/k^2$. Note that this definition of $\lambda$ in three-dimensional flow accords with the two-dimensional expression given in Dvorak (1969).

The full formula, $\lambda = D^2/ak^2$, for calculating $\lambda$ was used for parts A and C of the wing in Figure 12. $D^2$ is one square inch for 115 elements, or 645.16/115 square mm per element. $\lambda$ is, therefore 5.61/0.667=8.4 inasmuch as the roughness height in these areas is 1.0 mm and 0.667 is the ratio of the average roughness height to the maximum height. The lift loss is more sensitive to roughness height than roughness density so that slight errors in 'a' have little effect.